Online UV Curing of Electrospun Polysulfone Fibers Containing an Acrylate as Cross-Linker

On – line UV curing of electrospun polysulfone fibers containing an acrylate as crosslinker

Mian Farrukh Mehmood, Marco Sangermano*, Nonjabulo Prudence Gule,

Alberto Tiraferri, Peter E. Mallon

Mian Farrukh Mehmood

Department of applied science and technology,

Politecnico Di Torino
Corso Duca Degli Abruzzi 24, 10129, Torino Italy
E-mail: mian.mehmood@polito.it

*Marco Sangermano

Department of applied science and technology,

Politecnico Di Torino
Corso Duca Degli Abruzzi 24, 10129, Torino Italy
E-mail: marco.sangermano@polito.it

Nonjabulo Prudence Gule

Department of chemistry and polymer science

University of Stellenbosch, 7602 MATIELAND Stellenbosch, South Africa

E-mail: njabu@sun.ac.za

Alberto Tiraferri

Department of environment, land and infrastructure engineering

Politecnico Di Torino
Corso Duca Degli Abruzzi 24, 10129, Torino Italy
E-mail: alberto.tiraferri@polito.it

Peter E. Mallon

Department of chemistry and polymer science

University of Stellenbosch, 7602 MATIELAND Stellenbosch, South Africa

E-mail: pemallon@sun.ac.za

Abstract

To improve the functionality and the stability of electrospun nanofiber membranes (ENMs'), post electropsinning modification is often employed. In this work, we demonstrate a sustainable, *in-situ* UV–induced reactive electrospinning technique to produce solvent stable electrospun membranes in a single step operation. This approach is based on the addition of an acrylated crosslinker into the polysulfone-based dope solution and the online UV irradiation while it is electrospun thus ensuring reaction during the formation of the fibers. The feed solution was consisted of polysulfone, DMF, bisphenol A ethoxylate diacrylate and photo-initiator phenylbis-(2,4,6-trimethylbenzoyl) phosphine oxide. The electrospinning parameters and UV curing conditions were thoroughly optimized. Mats were also prepared via an offline approach in which UV curing was performed on the previously electrospun mats, and compared with the mats fabricated via the online curing method. The fibrous mats were characterized through ATR–FTIR, DSC, TGA and FESEM. As opposed to pristine polysulfone fibers, the electrospun mats

containing acrylate were stable in a variety of solvents, such as THF, acetone, ethyl acetate, DMSO, and toluene. The online irradiated mats of desired thickness were produced in a single step operation and the sustainability of the process was achieved through the optimization of electrospinning and solution parameters.

1. Introduction

Polysulfone (PSU) based porous polymeric membranes are extensively used for liquid separation, e.g., water and wastewater treatment, due to the ease of fabrication and high yield during production. PSU is one of the most common polymers employed to manufacture membranes because of its high glass transition temperature and absence of chemical groups. Conventional PSU membranes, developed through non solvent-induced phase separation, are typically used for ultrafiltration processes as well as support layers in thin-film composite membranes (TFC) applied for nanofiltration (NF), reverse osmosis (RO) and forward osmosis (FO) processes[1–3].

Recently, electrospun nanofiber membranes (ENMs') have been employed as successful replacements of conventional phase separation membranes because of low intrinsic porosity and lesser resistance to mass transport compared to traditional asymmetric membranes obtained by phase separation[4,5]. Several methodologies have been developed for the fabrication of high performance ENMs' including colloidal electrospinning of composite solutions[6–11], electrospinning of polymeric blends[12,13] and post-electrospinning modifications of the nanofibers[14–18]. Normally, post-electrospinning modification involves a chemical reaction between the polymer composing the membrane (nanofibers) and a multifunctional crosslinking reagent. This post-treatment strongly influences the membrane characteristics such as morphology, mechanical properties, and separation efficiency. More recently, alternate

methodologies to post-electrospinning modification have been developed, in which *in-situ* functionalization of ENMs' occurs during electrospinning. This approach is applied, for example, by the *in-situ* crosslinking of a curable feed solution during the spinning process. Such techniques are referred to as "reactive electrospinning". Reactive electrospinning ensures crosslinking by employing chemicals[19], UV radiations[20–24] and a combination of UV irradiation and pre[25] or post–heating[26].

It is worth noting that previous works on UV–induced reactive electrospinning, have mostly focused on biomedical application of nanofibers, such as tissue engineering and scaffolds, where scalable production is usually not anticipated. Therefore, these reports have not evaluated the sustainability of UV–induced electrospinning over a long time span. Moreover, previously reported works have not thoroughly investigated the effect of UV irradiation on the intra-fiber morphology.

In this work, we propose and develop solvent stable polysulfone electrospun membranes via UV-induced reactive electrospinning of PSU solution containing an acrylate resin as a crosslinker. The system ensures two simultaneous processes, i.e. radical polymerization of the acrylic monomer and the concurrent production of polysulfone nanofibrous mats. The UV irradiation is controlled in such a way that it irradiates only the nanofibers thus preventing the premature crosslinking of the acrylic resin and the phase separation of the polysulfone formulation. The feed solution is composed of PSU solution in DMF while bisphenol-A-ethoxylate diacrylate is employed as a crosslinker. The acrylic double bond conversion, electrospinning parameters (flow rate, applied voltage, distance from needle to collector) and UV curing behavior are investigated and optimized. The mats are also prepared via an offline UV curing method (post-electrospinning) and compared with the counterparts developed through online UV irradiation.

The electrospun mats are fully characterized using ATR–FTIR, DSC, TGA, and FESEM, while their porosity is estimated through the difference between the density of the feed solution and that of the obtained fibrous mats.

2. Experimental Section

2.1. Materials

Polysulfone (PSU, Mn=22,000 g mol^{-1}), solvent – N,N-Dimethyl formamide (DMF, anhydrous, 98.8%), and acrylic monomer bisphenol-A-ethoxylate (2EO/phenol) diacrylate (BEDA, average Mn=512 g mol^{-1} inhibited with 1000 ppm MEHQ) were purchased from Sigma–Aldrich. The photo initiator (PIn) phenylbis (2,4,6-trimethylbenzoyl) phoshineoxide (BAPO) was kindly provided by BASF.

2.2. Method

2.2.1. Preparation of electrospinning solutions

The pristine PSU solution was prepared in two different concentrations (15, 18 wt. %) in DMF by dissolving polymer granules with continuous stirring at 60 ^{o}C for seven hours followed by overnight cooling. All the feed solutions containing acrylic resin as crosslinker were prepared starting from PSU solutions at 18 wt. % and adding BEDA in three different concentrations, 5, 7 and 10 wt. % of the overall solution, and adding the photo initiator (PIn) Irgacure 819 at 5 wt. % with respect to the acrylic monomer. All the investigated formulations are shown in Table 1. To ensure homogenous solution, the formulations were sonicated for 20 min in an MRC ultrasonic bath DC 80H and kept at room temperature for at least 10 min to cool down before electrospinning.

2.2.2. Electrospinning protocol

Electrospinning was performed using a Genie plus Kent scientific horizontal electrospinning setup. All the electrospinning experiments were carried out using 10 mL syringes (Becton Dickinson Company, USA) and Sterican single-use hypodermic needles of gauge 0.60 mm (B Braun, USA). To determine the optimal concentration of pristine polysulfone, the flow rate was kept at 0.01 mL/min while distance to collector and applied voltage were changed in equal proportion to maintain the field strength as a constant. Thereafter all the solutions, both pristine PSU and PSU containing acrylate, were electrospun with 0.01 mL/min flow rate, 22 cm distance between needle and collector, and 30 KV applied voltage. All the electrospinning experiments were performed at temperature of 18–24 ^{o}C and relative humidity 40±5 %. The electrospun mats were collected on the static rectangular aluminum collectors of size 8 cm × 12 cm. Electrospinning was run to produce fibrous mat of thickness 120 ± 10 µm. To evaporate any residual DMF, the electrospun mats were kept in a fume hood for 24 hours prior to characterization and storage.

2.2.3. UV irradiation of electrospun fibers

The electrospun fibers, obtained from formulations containing BEDA as a crosslinker, were UV irradiated either online or offline. Both these curing operations were carried out using portable UV lamp Intelli-Ray 600 by Uvitron International USA, where the power of the lamp was adjustable from 35 to 100 %. The intensity was also controlled by adjusting the distance between the lamp head and the substrate.

The online UV irradiation was conducted on the polymeric solution while it was electrospun and before being collected. The UV irradiation was controlled to affect the convective flow only so the ohmic flow can have little or no impact of UV irradiation and solidification of electrospun

solution at the tip of needle could be avoided. A schematic representation of UV-induced reactive electrospinning is shown in Figure 1. The syringe was covered with black tape so the solution inside the syringe was never exposed to UV, thus preventing premature crosslinking of the acrylic monomer. The UV lamp intensity and its vertical distance from the needle were optimized to ensure continuous electrospinning and optimum crosslinking. For all the online UV irradiations, the power of lamp was kept at 60 %, since above this threshold the solution was found to solidify at the tip of the needle causing blockage.

The offline UV irradiation (post-electrospinning) was carried out by irradiating the already electrospun mats for 1 min with 100 % power of the lamp. This procedure was chosen for economical reasons, that is, the maximum extent of crosslinking was achieved in the minimum amount of time.

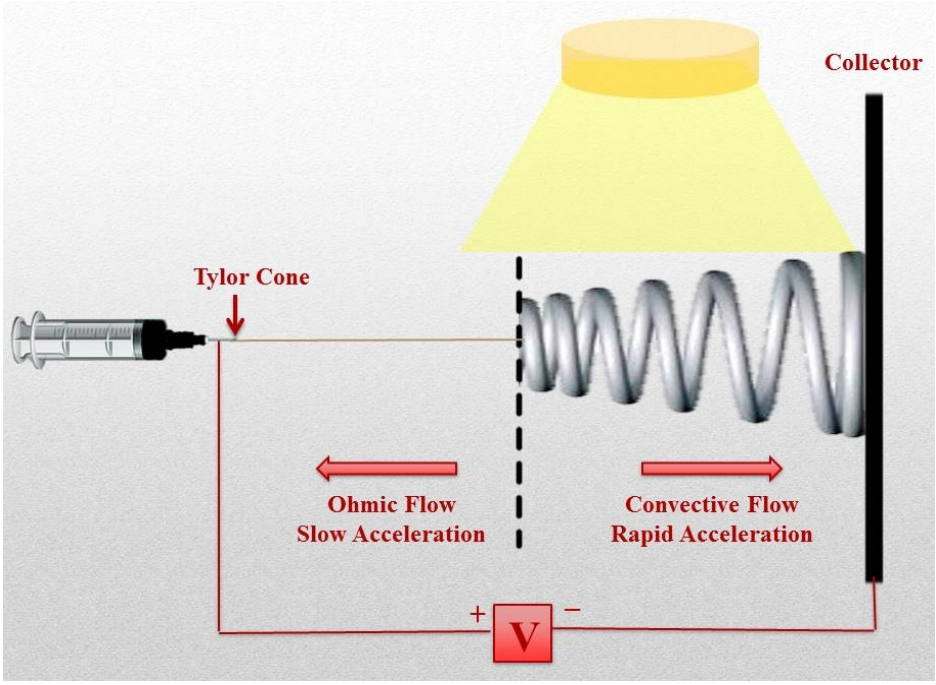

Figure 1. Schematic of the online UV-induced reactive electrospinning setup

Table 1: Composition of electrospinning solutions

Membrane Code	PSU wt. %	BEDA wt. %	PIn wt. % of BEDA	UV irradiation	
				Online	Offline
M00	18	-	-	-	-
M1F	18	5.0	5	✓	-
M1N	18	5.0	5	-	✓
M2F	18	7.0	5	✓	-
M2N	18	7.0	5	-	✓
M3F	18	10.0	5	✓	-
M3N	18	10.0	5	-	✓

2.3. Characterization of electrospun mats

2.3.1. Fourier transform infrared spectroscopy analysis (FTIR)

The spectrophotometer Thermo Scientific Nicolet iS10, equipped with attenuated total reflectance (ATR) accessory containing a diamond crystal internal reflection element, was used for Fourier transform infrared spectroscopy (FTIR) and attenuated total reflectance Fourier transform infrared spectroscopy (ATR – FTIR) analysis. To evaluate the crosslinking extent of pure acrylic monomer, the monomer was cast on a silicon wafer and analyzed with FTIR before and after UV irradiation. The analysis was carried out with a resolution of 4 cm^{-1} and 32 scans in the wavenumber range between 650 cm^{-1} and 4000 cm^{-1}. The conversion of acrylic double bonds was calculated by following the decrease of the peak area of C=C at 810 cm^{-1} normalized with the peak area of C=O at 1730 cm^{-1}. The crosslinking of electrospun mats was evaluated with ATR–FTIR analysis. The parameters during analysis and the target peaks were the same as discussed above for the pure acrylic monomer.

2.3.2. Differential scanning calorimetry (DSC)

The glass transition temperatures of pure polymer and its blends with the acrylic resin were obtained using a differential scanning calorimetry (TA Instrument DSC Q 200) in a nitrogen atmosphere. Almost 8 mg of each fibrous mat was encased in an aluminum sample pan and heated from 0 to 260 ^{o}C at ramp temperature rate 10 ^{o}C/min, followed by a cooling to 0 ^{o}C at 5 ^{o}C/min, and by second heating to 260 ^{o}C at 10 ^{o}C/min.

2.3.3. Thermal gravimetric analysis (TGA)

The thermal degradation characteristics of the fibers of pure PSU and its blends were obtained using thermogravimetric analysis (TA instruments TGA Q500) in a nitrogen atmosphere. Approximately 8 mg of each fibrous mat was heated from 20 to 600 ^{o}C at a rate of temperature increase of 10 ^{o}C/min.

2.3.4. Morphological analysis

Qualitative morphological evaluation of the fibers was carried out with an optical microscope, OLYMPUS CX31 by Wirsam Scientific, for the optimization of electrospinning parameters. Detailed morphology and diameter of all fibers was analyzed through field emission scanning electron microscopy (FESEM) at an accelerating voltage 5 KV. The InLens images were obtained using a Zeiss MERLIN FEG® scanning electron microscope equipped with state of the art GEMINI II® column ensuring the good control of spot and current. The absence of beads was confirmed at magnification 10K and pores on the surface of individual fiber were evidently shown at magnification 20K. The samples were prepared by affixing a small rectangular piece of electrospun membrane on the sample stand using carbon tape. Prior to imaging, all the samples were gold coated up to a thickness of 10 nm using Edward S150A sputter coater. The fiber

diameters were measured directly from the images using software Carl Zeiss Axio vision LE and an average value was calculated from 60 fibers from different SEM micrographs.

2.3.5. Porosity

An approximate estimation of the mat porosity was collected through the difference in density between the feed solution and the fibers. The density of the feed solution (ρs) was obtained by weighing 1 mL of feed solution with careful measurement of solution volume using a calibrated Rainin micropipette. The bulk density of fibrous (ρf) mats was calculated by weighing a mat of size 1 cm × 1 cm. The thickness of all fibrous mats was obtained with a calibrated micrometer having resolution of 1 μm. The resultant porosity (Φ) was calculated as,

$$\Phi\ (\%) = \left[1 - \frac{\rho f}{\rho s}\right] 100$$

2.3.6. Solvent resistance assessment

The solvent resistance of the crosslinked polysulfone membranes was assessed by immersing cutouts of the membrane in various solvents. The immersion was carried out at room temperature for at least 120 hours. A qualitative evaluation was made based on the visual inspection of the membranes following this protocol. The resultant membranes were categorized into three grades: 1) stable 2) swollen 3) dissolved in the specific solvent.

3. Results and discussion

This study presents the fabrication and characteristics of PSU nanofibers produced by electrospinning in the presence of an acrylic crosslinker, with the aim to obtain solvent stable

mats that may be used as stand-alone or support layers for liquid and gas separation. The fiber morphology and diameters resulting from electrospinning are influenced by the type of polymer, its concentration, the viscosity of solution, the type of solvent, the needle gauge, the applied voltage, the feed rate and the distance to collector[27]. Ambient parameters, such as temperature and relative humidity, also affect significantly the characteristics of the resultant fibers[28]. In addition to studying the effect of aforementioned parameters, we have also investigated how UV irradiation influences the fiber morphology when UV curing is performed either online (during electrospinning) or offline (post-electrospinning).

3.1. Effect of solution and electrospinning parameters for pristine PSU

The pristine PSU solutions were electrospun over a wide range of electrospinning parameters, to optimize the protocol and to minimize the formation of beads. The solutions investigated along with electrospinning parameters are given in Table 2. The feed solution containing 15 wt. % of PSU produced beads under all the combinations of electrospinning parameters, while the solution containing 18 wt.% PSU resulted in bead free fibers in most of the cases. Figure 2 shows representative SEM micrographs of the electrospun fibers for the solution containing 15 wt. % (solution B) and 18 wt. % (solution D), respectively. The resultant fiber diameter increased with the increase of PSU concentration, in accordance with previous reports[6,10]. Furthermore, the fiber diameter decreased with the increase of needle-to-collector distance. This result is explained by the well-known drawing effect.

Table 2. Influence of concentration and parameters on fibers' morphology and diameter

No.	wt. % of PSU	Flow rate [ml/min]	Distance [cm]	App. Voltage [KV]	Fiber Dia. [nm]	Resultant morphology
A	15	0.01	15	20	570	Beads
B	15	0.01	22	30	352	Beads
C	18	0.01	15	20	2100	No beads
D	18	0.01	22	30	994	No beads

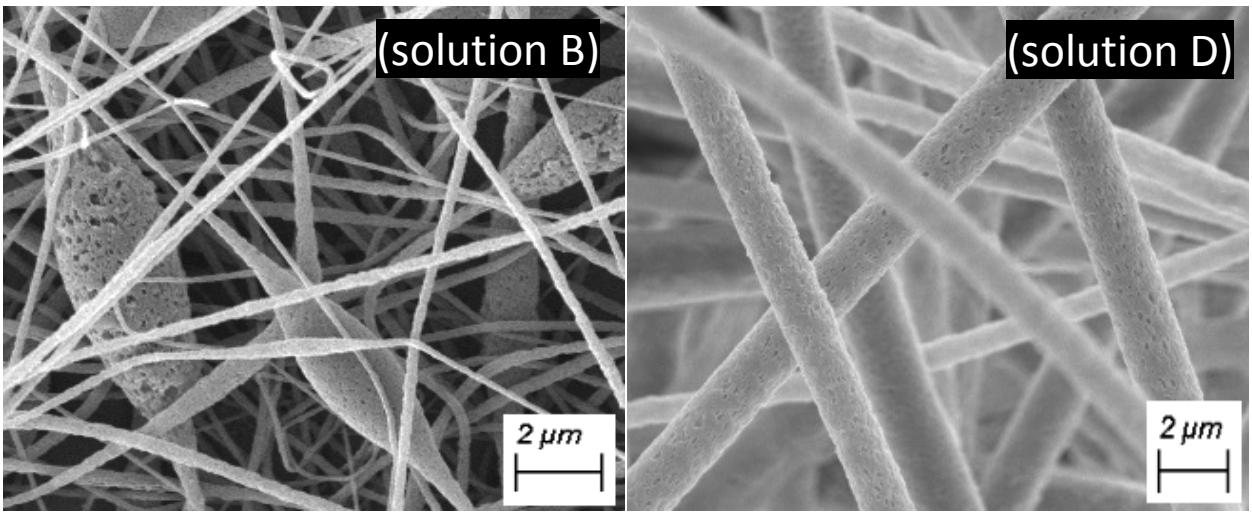

Figure 2. SEM images of pristine polysulfone fibers obtained from solution B (15 wt. % of PSU) and solution D (18 wt. % of PSU)

3.2. Influence of UV irradiation on the PSU based solutions containing BEDA crosslinker

The UV irradiation conditions were optimized for the pristine BEDA monomer before investigating the effect of UV curing on the electrospun mats. The acrylic double bond conversion of the monomer was evaluated through FTIR analysis by following the decrease of the C=C peaks 810 cm^{-1} normalized with the peak C=O centered at 1730 cm^{-1} (Figure 3). An average conversion of 85 % was achieved after one minute of irradiation. These results were

used to adjust the UV curing parameters of the PSU solutions containing the acrylate as crosslinker.

The solutions containing the acrylate were UV cured either online, during the electrospinning process, or offline, soon after electrospinning. Both the online and the offline cured fibers were analyzed by ATR–FTIR to determine the degree of curing. As an example, spectra for the formulations containing 10 wt. % of BEDA are shown in Figure 4. The calculated degrees of acrylic double bond conversion of PSU fibrous mats, containing 5, 7, and 10 wt. % BEDA and irradiated online, were 85, 82, and 80% respectively. While fibrous mats, obtained from the same solutions but cured offline, exhibited acrylic double conversion degrees of 85, 85, and 82%, respectively. Therefore, comparable degrees of acrylic double bond conversion can be achieved through either the online or the offline process. However, the online irradiation process allowed obtainment of defect-free crosslinked electrospun nanofibrous membranes in a more facile and sustainable single step operation.

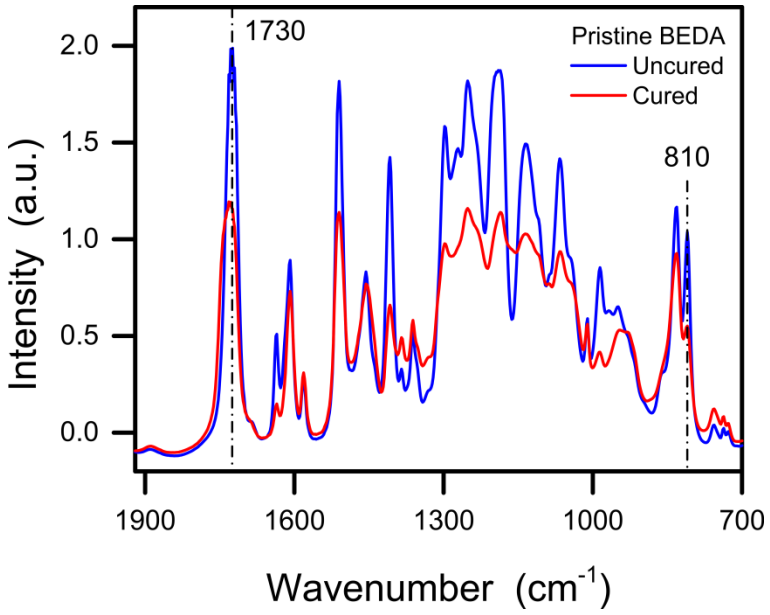

Figure 3. FTIR spectra of pristine BEDA before and after UV curing

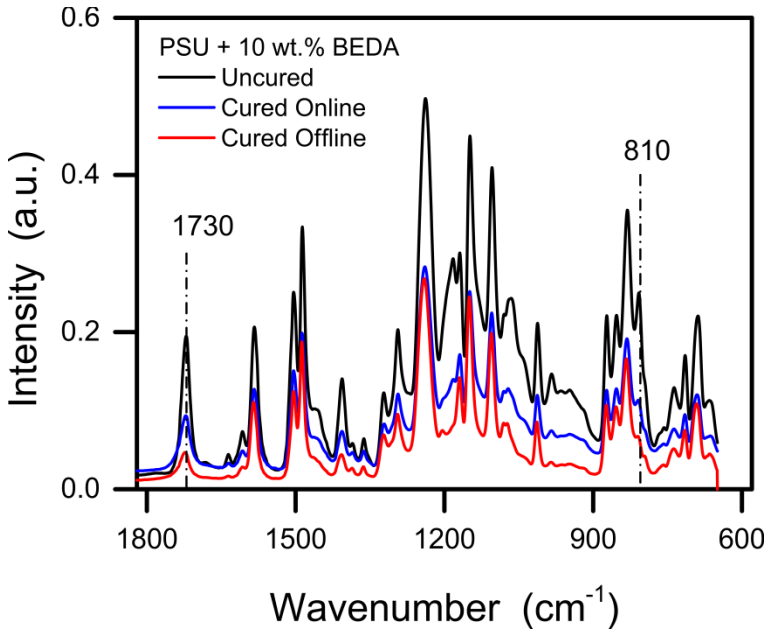

Figure 4. ATR – FTIR spectra of PSU electrospun fibers, containing 10 wt. % of BEDA, before curing and after online or offline curing

3.3. Morphological analysis

Representative SEM micrographs are presented in Figure 5 together with the respective fiber diameter distributions. Fibers of electrospun membranes obtained from pristine PSU (solution concentration of 18 wt. %) were free of beads (Figure 5a) and had an average dimension of 994 nm with standard deviation of 275 nm. Moreover, the fibers showed surface pores, which may be the result of non-solvent induced phase separation (NIPS) as a result of the exchange of DMF with the moisture present in the air. A similar intra-fiber structure, resulting from NIPS, was reported by others[29] during fabrication of porous polystyrene fibers.

The morphology of the PSU fibers, obtained in the presence of BEDA crosslinker are shown in Figures 5b–e. All these fibers are free of beads, thanks to careful control of the UV-induced reactive electrospinning. With online irradiation, the fiber diameter from solution of PSU + 5 wt.

% BEDA was 392±229 nm, while that from PSU + 10 wt. % BEDA was 409±253 nm. An increase of diameter with increased acrylic content may be associated with the higher viscosity of the solution containing larger amount of monomer. A similar trend was observed with offline irradiated mats, for which the fiber diameters were 509±179 nm for mats obtained from solutions of PSU + 5 wt. % BEDA and 579±183 nm for those spun from PSU + 10 wt. % BEDA. In general, the size of the fibers achieved in the presence of BEDA crosslinker was lower than that obtained using pure PSU. Interestingly, offline irradiated fibers' diameter were slightly higher but had narrower diameter distribution than those resulting from irradiating the polymer online. Conducting curing during fiber formation may change slightly the electrospinning conditions, possibly due to the added energy flux from the UV light irradiating the samples and the effects of the rate of solvent evaporation. Overall, cross-linked mats obtained from online and offline curing were similar in terms of morphological properties.

The presence of surface pores on the fibers was found to be influenced by the weight percentage of acrylate and mode of UV curing. For instance, PSU electrospun fibers containing 10 wt. % BEDA, UV cured either online or offline, were generally found to be deprived of surface pores (Figure 5c,e). On the contrary, fibers obtained from solution containing 5 wt. % of BEDA and cured offline retained surface pores (Figure 5d) while the online irradiated fibers, having similar formulation, couldn't retain those peculiar pores (Figure 5b). This result may be rationalized with the higher extent of DMF removal during the continuous online UV irradiation process, which reduced the amount of non-solvent exchangeable with ambient moisture.

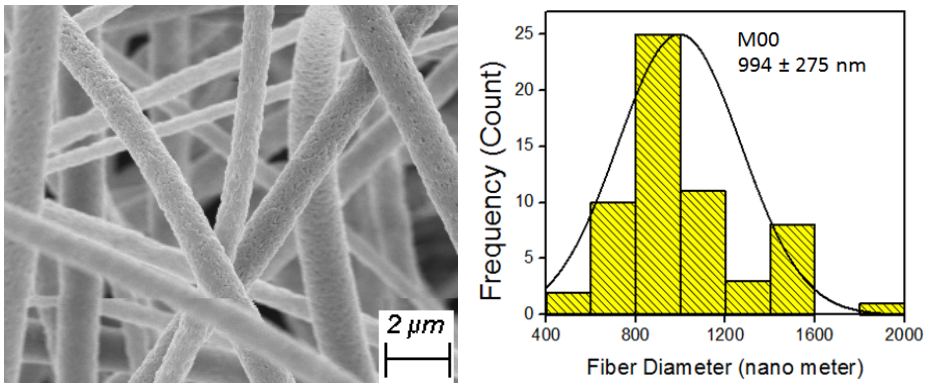

Figure 5a. SEM image and diameter distribution of pristine PSU fibers

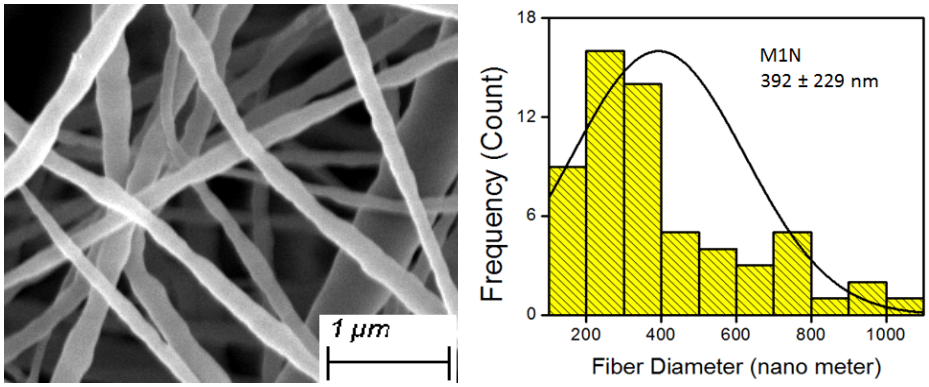

Figure 5b. SEM image and diameter distribution of fibers obtained in the presence of 5 wt. % BEDA cured online

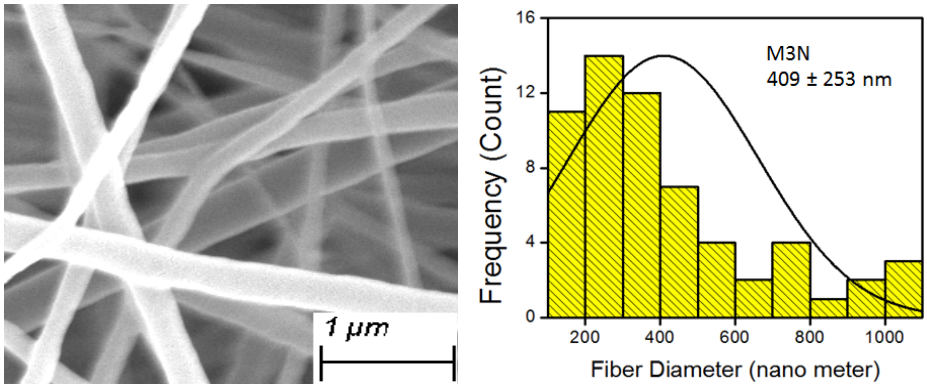

Figure 5c. SEM image and diameter distribution of fibers obtained in the presence of 10 wt. % BEDA cured online

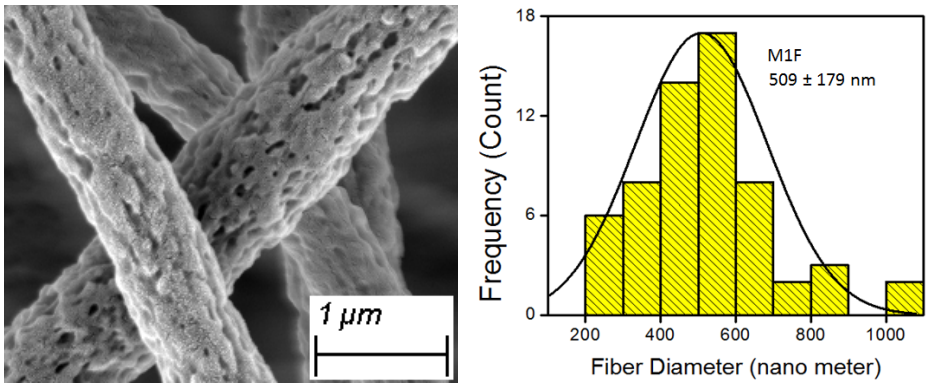

Figure 5d. SEM image and diameter distribution of fibers obtained in the presence of 5 wt. % BEDA cured offline

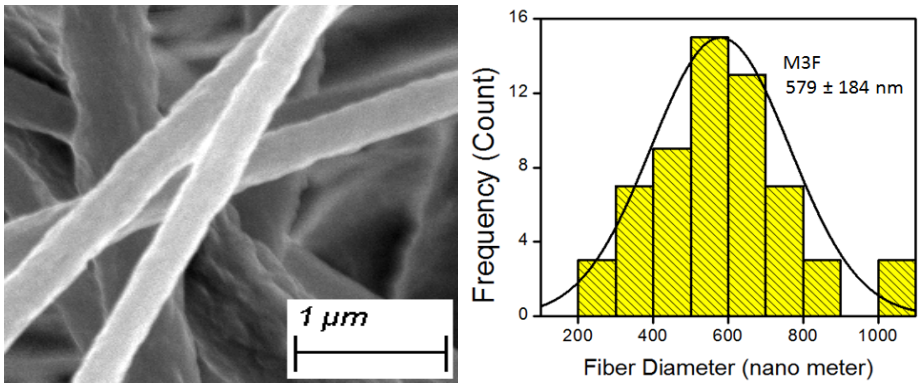

Figure 5e. SEM image and diameter distribution of fibers obtained in the presence of 10 wt. % BEDA cured offline

Figure 6 shows the estimated macro porosity of the fibrous mats. The offline irradiated mats had somewhat higher porosity in comparison to the mats obtained by irradiating fibers online: the mats obtained from PSU containing 10 wt. % BEDA exhibited highest porosity.

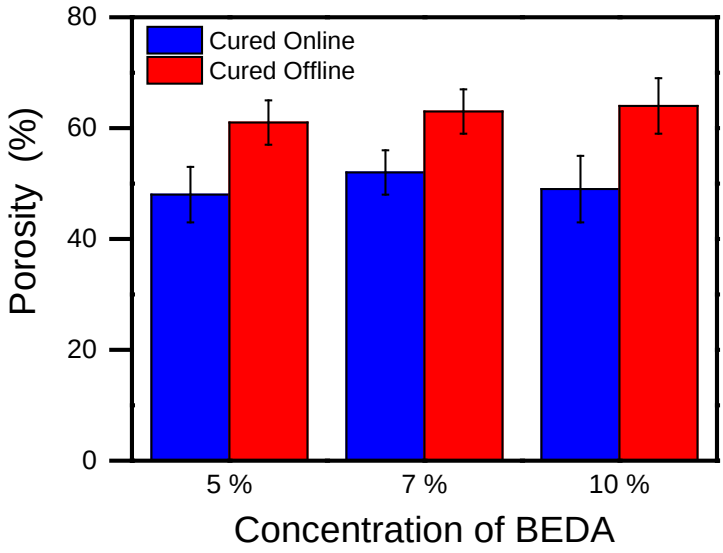

Figure 6. Porosity of different electrospun nanofibrous membranes

3.4. Thermal characterization of electrospun fibrous membranes

The DSC curves for online and offline UV-cured mats are shown in Figure 7 and compared to the pristine PSU electrospun mats. The pristine PSU fibers exhibited Tg centered around 190 ^{o}C, in accordance with the reported Tg value of pristine PSU[30]. Two distinct Tg values are evident from the DSC analysis of fibers obtained from PSU solutions containing 10 wt. % of BEDA crosslinker. The first Tg, at around 90 ^{o}C, is ascribed to BEDA, while the second Tg at 170 ^{o}C may be attributed to the PSU. The incorporation of low molecular weight BEDA resin resulted in drop of PSU Tg from 190 to 170 ^{o}C. Similar behavior was observed in our previous work where BEDA functionalized PSU membranes were developed through NIPS[31]. The thermal properties of fibers showed no significant difference between online and offline irradiation. This result is in accordance with similar acrylic double bond conversion achieved for the two methodologies.

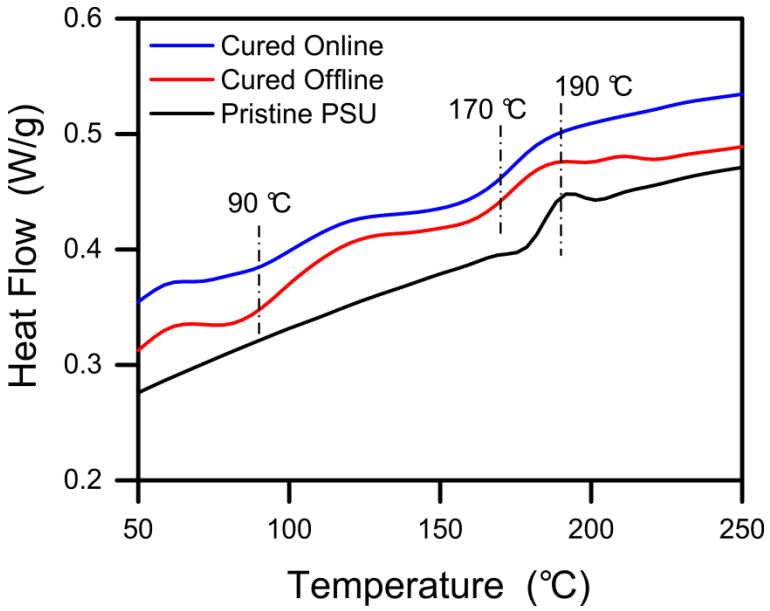

Figure 7. DSC curves of pristine PSU mats and of mats obtained in the presence of 10 wt.% BEDA, UV-cured online and offline

TGA analysis was performed in order to assess the thermal stability of electrospun mats. The results are shown in Figure 8. The pristine PSU was found to undergo single step degradation at 530 ^{o}C, while double-step degradation was observed for the fibers obtained in the presence of BEDA. The first degradation step at lower temperature may be attributed to the BEDA network degradation at around 420 ^{o}C, followed by PSU degradation around 510 ^{o}C. Also in this case, the thermal degradation behavior of the online and offline cured samples were similar and only the results of online cured system are presented here.

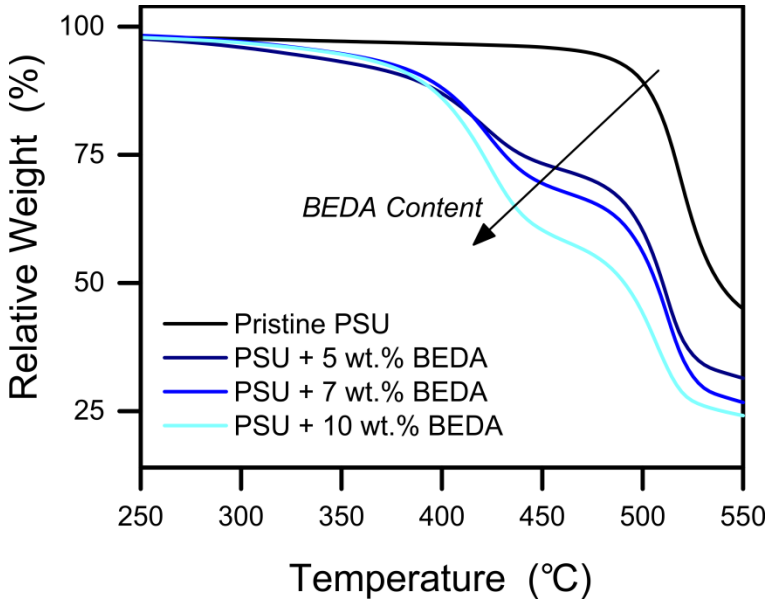

Figure 8a. TGA curves of pristine PSU and online cured fibers obtained in the presence of BEDA crosslinker

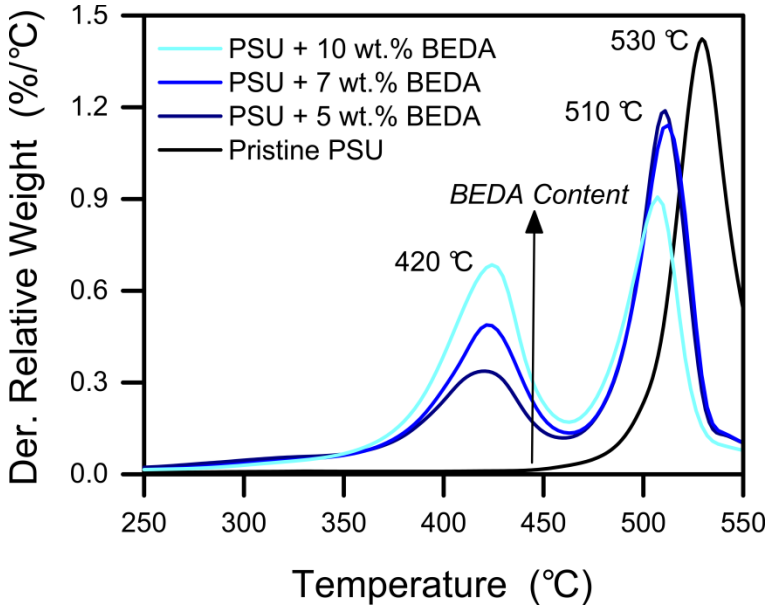

Figure 8b. DTGA of pristine PSU and online cured fibers obtained in the presence of BEDA crosslinker

3.5. Solvent stability of membranes

To confirm the solvent stability of the UV cured acrylic functionalized PSU electrospun nanofibrous membranes, both reference (pristine PSU) and modified membranes were immersed in different solvents at room temperature. A qualitative analysis was carried out after 120 hours of immersion and the results are summarized in Table 3. Membranes made from solutions of pristine PSU were dissolved or swollen in all the tested solvents. By increasing the concentration of BEDA, thus the extent of crosslinking in the matrix, electrospun fibers became more chemically robust. The most resistant formulations were based on PSU containing 10 wt. % of BEDA crosslinker, which were found to be stable in THF, acetone, ethyl acetate, DMSO, and toluene. This finding is in accordance with our previous work on solvent stable acrylic functionalized PSU membranes developed through NIPS[31].

Table 3. Solvent stability of pristine and modified PSU ENMs'

Solvent	M00	M1N	M1F	M2N	M2F	M3N	M3F
THF	1	1	1	×	×	0	0
Acetone	×	0	0	0	0	0	0
Ethyl acetate	×	0	0	0	0	0	0
DMSO	1	×	×	×	×	0	0
Toluene	1	0	0	0	0	0	0

0–stable, 1–dissolved, ×–Swelling

4. Conclusion

In this paper, electrospun nanofiber membranes (ENMs') were fabricated via a reactive electrospinning method where on-line UV curing of a PSU based solution containing an acrylate crosslinker was performed. For comparison, the ENMs' were also prepared with offline UV irradiation method, in which curing was carried out after formation of the fibrous mats. The sustainability of online irradiation was achieved through optimization of UV curing and electrospinning parameters. The near-complete crosslinking reaction of acrylic resin in the fibers was confirmed with ATR–FTIR. Full thermal analysis of the electrospun membranes was performed, as well as morphological characterization. Tests revealed that fiber diameter decreased in the presence of the crosslinking agent compared to the pure polymer, that higher content of crosslinker produced slightly larger distribution of fiber diameters, and finally that offline irradiated fibers had slightly larger but overall similar diameter to fibers produced via online irradiation. All the crosslinked membranes were comparable in terms of thermal properties and chemical resistance, regardless of the protocol followed for UV irradiation. Solvent stability induced by the presence of the crosslinker in the electrospun solution was excellent in all cases. These results suggest that the online UV curing method is an effective and more convenient approach to customize fiber properties during electrospinning compared to post-fabrication strategies. Modified ENMs' may serve the purpose of solvent-stable separation membranes or support layers in gas or liquid separation processes, such as ultrafiltration, reverse osmosis, perevaporation, and forward osmosis.

Keywords: Polysulfone, acrylic functionalization, reactive electrospinning, solvent stability

References

1. Yang Zhang, Min Guo, Guoyuan Pan, Hao Yan, Jian Xu and Yuanteng Shi, *J. Membr. Sci*. **2015,** *476*, 500.

2. Byeong-Heon Jeong, Eric M.V. Hoek, Yushan Yan, Arun Subramani, Xiaofei Huang and Gil Hurwitz, *J. Membr. Sci*. **2007,** *294*, 1.

3. Alberto Tiraferri, Ngai Yin Yip, William A. Phillip, Jessica D. Schiffman and Menachem Elimelech, *J. Membr. Sci*. **2011,** *367*, 340.

4. Yoon, K. Kim, K. Wang, X. Fang, D. Hsiao and B. S. Chu, *Polymer* **2006,** *47*, 2434.

5. Subramanian, S and Seeram, R, *Desalination* **2013,** *308*, 198**.**

6. M. Obaid. Gehan M.K. Tolba, Moaaed Motlak, Olfat A. Fadali, Khalil Abdelrazek Khalil, Abdulhakim A. Almajid, Bongsoo Kim and Nasser A.M. Barakat, *Chem. Eng. J.* **2015**, *279*, 631.

7. M. Obaid, Zafar Khan Ghouri, Olfat A. Fadali, Khalil Abdelrazek Khalil, Abdulhakim A. Almajid and Nasser A. M. Barakat, *ACS Appl. Mater. & Interfaces* **2016,** *8*, 4561.

8. Ming Hang Tai, Peng Gao, Benny Yong Liang Tan, Darren D. Sun and James O. Leckie, *ACS Appl. Mater. Interfaces* **2014,** *6*, 9393.

9. Shuai Jiang, Beatriz Chiyin Ma, Jonas Reinholz, Qifeng Li, Junwei Wang, Kai A. I. Zhang, Katharina Landfester and Daniel Crespy, *ACS Appl. Mater. Interfaces* **2016,** *8*, 29915.

10. M. Obaid, Nasser A.M. Barakat, O.A. Fadali, Moaaed Motlak, Abdulhakim A. Almajid and Khalil Abdelrazek Khalil, *Chem. Eng. J.* **2015,** *259*, 449.

11. Jiajia Xue, Yuzhao Niu, Min Gong, Rui Shi, Dafu Chen, Liqun Zhang and Yuri Lvov, *ACS Nano* **2015,** *9(2),* 1600.

12. Alexis Wagner, Vida Poursorkhabi, Amar K. Mohanty and Manjusri Misra, *ACS Sustainable Chem. Eng.* **2014,** *2*, 1976.

13. Andreia F. de Faria, Francois Perreault, , Evyatar Shaulsky, Laura H. Arias Chavez and Menachem Elimelech, *ACS Appl. Mater. Interfaces* **2015,** *7*, 12751.

14. Hee Joong Kim, Min-Young Lim, Kyung Hwa Jung, Dong-Gyun Kima and Jong-Chan Lee, *J. Mater. Chem.* A **2015,** *3*, 6798.

15. Jianqiang Wang, Pan Zhang, Bin Liang, Yuxuan Liu, Tao Xu, Lifang Wang, Bing Cao and Kai Pan, *ACS Appl. Mater. Interfaces* **2016,** *8*, 6211.

16. H. j. Cho, S.K. Madhurakkat, J. h. Lee, J. Lee, K. M. Lee, C.S. Shin and H. Shin, *ACS Appl. Mater. Interfaces* **2014,** *6*, 11225.

17. X. Wang, S. Yuan, D. Shi, Y. Yang, T. Jiang, S. Yan, H. Shi, S. Luan and J. Yin, *Appl. Surf. Sci.* **2016,** *375*, 9.

18. Qiuxia Fu, Xueqin Wang, Yang Si, Lifang Liu, Jianyong Yu, and Bin Ding, *ACS Appl. Mater. Interfaces* **2016,** *8(18)*, 11819.

19. Christina Tang, Carl D. Saquing, Jonathon R. Harding and Saad A. Khan, *ACS Macromolecules* **2010,** *43*, 630.

20. Hong -Wei He, Le Wang, Xu Yan, Li-Hua Zhang, Miao Yu, Gui-Feng Yu, Rui-Hua Dong, Lin-Hua Xia, Seeram Ramakrishna and Yun-Ze Long, *RSC Adv.* **2016,** *6*, 29423.

21. Wei-Han Lin and Wei-Bor Tsai, *Biofabrication* **2013,** *5(035008)*, 1.

22. Heyun Wang, Yakai Feng, Wencheng Zhang, Minglin Sun. Zichen Fang, Wenjie Yuan and Massuri Khan, *J Mater Sci: Mater Med* **2012,** *23*, 1499.

23. Seong Han Kim, Sae-Hoon Kim, Sujith Nair and Eric Moore, *ACS Macromolecules* **2005,** *38*, 3719.

24. Pankaj Gupta, Scott R. Trenor, Timothy E. Long and Garth L. Wilkes, *ACS Macromolecules* **2004,** *37*, 9211.

25. Xiaoming Xu, Jian-Feng Zhang and Yuwei Fan. *ACS Biomacromolecules* **2010,** *11*, 2283.

26. Emre Bastürk, Burcu Oktay and Memet Vezir Kahraman , *J Polym. Res.* **2015,** *22(7)*, 1.

27. Shin, Y. Hohman, M. Brenner and M. Rutledge, G, *Appl. Phys. Lett.* **2001,** *78(8)*, 1149.

28. Megelski, S. Stephens, J. S. Chase, D. B. Rabolt and J. F. Microand, *ACS Macromolecules* **2002,** *35(22)*, 8456.

29. Jinyou Lin, Bin Ding, Jianmao Yang, Jianyong Yu and Gang Sunf, *Nanoscale* **2012,** *4*, 176.

30. M. Sangermano, M. Mian Farrukh, A. Tiraferri, C. Dizman, Y. Yagci, *Mater. today commun.* **2013,** *5*, 64.

31. Mehmood Mian Farrukh, Paula Bosch, Mattia Giagnorio, Alberto Tiraferri, Marco Sangermano, *Polym. Int.* **2017,** *66*, 64.

Graphical Abstract

On – line UV curing of electrospun polysulfone fibers containing an acrylate as crosslinker

Mian Farrukh Mehmood, Marco Sangermano*,

Nonjabulo Prudence Gule, Alberto Tiraferri, Peter E. Mallon